Research Article

Diego del Olmo*, Michal Pavelka, and Juraj Kosek

Open-Circuit Voltage Comes from Non-Equilibrium Thermodynamics

Abstract: Originally derived by Walther Nernst more than a century ago, the Nernst equation for the open-circuit voltage is a cornerstone in the analysis of electrochemical systems. Unfortunately, the assumptions behind its derivation are often overlooked in the literature, leading to incorrect forms of the equation when applied to complex systems (for example, those with ion-exchange membranes or involving mixed potentials). Such flaws can be avoided by applying a correct thermodynamic derivation independently of the form in which the electrochemical reactions are written. The proper derivation of the Nernst equation becomes important, for instance, in modeling of vanadium redox flow batteries or zinc-air batteries. The rigorous path towards the Nernst equation derivation starts in non-equilibrium thermodynamics.

Keywords: redox flow batteries, open-circuit voltage, non-equilibrium thermodynamics, Zn-air battery

1 Introduction

"Thermodynamics is a funny subject. The first time you go through it, you don't understand it at all. The second time you go through it, you think you understand it, except for one or two points. The third time you go through it, you know you don't understand it, but by that time you are so used to the subject, it doesn't bother you anymore." (Arnold Sommerfeld)

The open-circuit voltage (OCV) is generally defined as the voltage between the terminals of an electrochemical cell when no current flows through the cell. As it can be measured directly, it is used as a control tool in electrochemical energy storage devices (e. g., as a state-of-charge estimator [1] or to identify undesired processes taking place in the system [2]). However, to properly interpret the measured value, a formula relating it to the cell properties is required: the so-called Nernst equation.

Although it was Helmholtz who first derived a formula relating voltage and dissolved species concentrations [3], Nernst formulated the relation in a general thermodynamic way: the Gibbs energy of the overall reaction (written down with no charge imbalance) will be equal to the maximal electrical work that can be obtained (cf. [4, 5]), which determines the OCV. In general, it is sufficient to consider only the reaction coefficient and standard potentials of both half-cell reactions (associated to the liquid-solid interfaces at both electrodes) to derive a formula for the OCV. The Donnan potential and other membrane-related effects are added afterwards; see, e. g., [6]. Let us refer to this way toward the Nernst relation as the simplified derivation. However, for more complex systems, like those using ion-exchange membranes, this simplified procedure does not always lead to the correct OCV and a more careful derivation considering all interfaces present in the system is required [7]. It is common in the literature that the simplified derivation leads to incorrect forms of the Nernst

*Corresponding author: Diego del Olmo,** Department of Chemical Engineering, University of Chemistry and Technology Prague, Technická 5, 16628 Prague 6, Czech Republic, e-mail: delolmod@vscht.cz
Michal Pavelka, Department of Chemical Engineering, University of Chemistry and Technology Prague, Technická 5, 16628 Prague 6, Czech Republic; and Mathematical Institute, Faculty of Mathematics and Physics, Charles University in Prague, Sokolovská 83, 186 75 Prague 6, Czech Republic, e-mail: pavelka@karlin.mff.cuni.cz, ORCID: https://orcid.org/0000-0003-0605-6737
Juraj Kosek, Department of Chemical Engineering, University of Chemistry and Technology Prague, Technická 5, 16628 Prague 6, Czech Republic, e-mail: Juraj.Kosek@vscht.cz

equation. In such cases, the proper thermodynamic derivation of the Nernst equation provides a careful way that directly contains all necessary effects.

Note that the OCV (or at least its typically measurable value) does not correspond with the complete thermodynamic equilibrium of the cell. Imagine an electrochemical cell whose electrodes are abruptly disconnected. The voltage between the electrodes would first equilibrate at some value (the first plateau in the voltage/time curve [7]), which is interpreted as the OCV. When, however, one keeps waiting, the voltage can change further as other effects take place (e. g., species crossover or parasitic reactions). The complete equilibrium given by the global minimum of Gibbs energy (see, e. g., [8]) would be characterized by a different value, which usually would not correspond with the measured OCV. We focus on the operational definition of the OCV that is given by the first plateau in the voltage/time curve, which means that we only consider the relaxation of the most relevant processes. Such analysis requires the application of both equilibrium and non-equilibrium thermodynamics.

This work comprehensively reviews the derivation of the Nernst equation from basic thermodynamics. Furthermore, we show how the use of simplified derivations can lead to incorrect interpretations of the OCV for complex systems. Special cases in which multiple reactions can take place at one electrode leading to mixed potentials (e. g., corrosion processes) are also discussed in terms of non-equilibrium thermodynamics. Finally, we identify recent developments for which this thermodynamic derivation can be particularly relevant. The novelty of this work does not, of course, lie in the Nernst equation itself, but in recalling the principles behind it in nowadays thermodynamic terminology and in careful application of the principles in particular systems (zinc-air and all-vanadium), including non-equilibrium processes. It is shown that for instance in vanadium and zinc-air redox flow batteries the thermodynamic derivation of Nernst relation gives better results than the simplified one.

2 Thermodynamics origin of the open-circuit voltage

Let us first recall a few fundamental concepts of equilibrium and non-equilibrium thermodynamics and physical chemistry, namely, electric potential, electrochemical potential, electrochemical affinity, and OCV.

2.1 Electric potential

The electrochemical potential of species α in a solution can be generally expressed as the sum of the chemical potential μ_α and the molar electrostatic potential energy [9] such that

$$\tilde{\mu}_\alpha = \mu_\alpha + z_\alpha F\varphi = \mu_\alpha^\circ + RT \ln \left(\underbrace{\gamma_\alpha \frac{b_\alpha}{b^\circ}}_{a_\alpha} \right) + z_\alpha F\varphi, \tag{1}$$

where $\tilde{\mu}_\alpha^\circ$ is the standard chemical potential of the species α (here in aqueous solution), b_α is its molality (b° the standard molality), γ_α is its activity coefficient, a_α is its activity, z_α is the charge number, and φ is the electrostatic Maxwell potential, for which the Poisson equation holds in electrostatics; see, e. g., [10, 5].

The potential measured by a potentiometer is proportional to the difference in electrochemical potential of electrons between the terminals (measuring electrodes). The electrochemical potential of electrons is defined as

$$\tilde{\mu}_{e^-} = -F\Phi, \tag{2}$$

which should be also regarded as the definition of electric potential Φ; see [10, 11, 7] for more details.

Note that, in general, the potentials φ and Φ are different. The difference can be demonstrated on contact of two metals with different Fermi energies. In equilibrium, the electrochemical potentials of electrons in the two metals are equal, thus Φ is the same in both metals, whereas the Maxwell (or electrostatic) potentials φ in the two metals are different, which compensates the difference in the Fermi energies. Moreover, it is the electrostatic potential φ (not Φ) for which the Poisson equation holds.

2.2 Electrochemical reactions

Electrochemical reactions are driven by differences in electrochemical affinities,

$$\tilde{\mathcal{A}}_r = \sum_\alpha \nu_{r\alpha} \tilde{\mu}_\alpha, \tag{3}$$

where the electrochemical potentials $\tilde{\mu}_\alpha$ are evaluated near the electrode surfaces; see, e. g., [12, 13]. The equilibrium of an electrochemical reaction is then characterized by vanishing electrochemical affinity,

$$\sum_\alpha \nu_{r\alpha} \tilde{\mu}_\alpha = 0. \tag{4}$$

2.3 Transport

The flux of species α is typically proportional to the gradient of electrochemical potential of the species,

$$\mathbf{j}_\alpha = -\mathcal{D}_\alpha \nabla \tilde{\mu}_\alpha; \tag{5}$$

see, e. g., [14, 5], where this relation is derived from microscopic theory. For infinitely dilute solutions $\mathcal{D}_\alpha = D_\alpha \cdot c_\alpha / RT$, where D_α is the diffusion coefficient.

  Considering transport through a membrane, there is no net flux if the electrochemical potential of the transported species is the same on both sides of the membrane (neglecting possible coupling and crossover effects),

$$\tilde{\mu}_\alpha^P = \tilde{\mu}_\alpha^N, \tag{6}$$

where P and N stand for the positive and negative sides, respectively.

  Let us now discuss transport in battery electrolytes. According to eq. (1), the gradient of $\tilde{\mu}_\alpha$ can be split into the gradient of chemical potential μ_α, which depends on the molalities of the species α in the mixture, and the gradient of the Maxwell potential φ. Assuming perfect mixing (homogeneous concentrations, i. e., $\nabla c = 0$), the condition of zero flux becomes a condition of zero gradient of Maxwell electrostatic potential,

$$\nabla \varphi = 0. \tag{7}$$

Let us now comment more on this equation. If there were non-zero gradients of electrochemical potentials, there would be some fluxes (proportional to the gradients), which is in contradiction with our assumption of quasi-stationary state. The electrochemical potentials can be split into their chemical and electrical contributions (1). The assumption of perfect mixing means that there are no gradients of concentrations within the electrolytes (or that they are negligible). The electrical contributions to the electrochemical potentials have thus zero gradients as well. The Maxwell electrostatic potential can be thus considered constant within the electrolyte (assuming no net fluxes and perfect mixing). Consequently, we assume that the electrochemical potential of species in the electrolyte is the same near the membrane and near the electrode, which greatly simplifies the modeling (since the Poisson equation would have to be solved otherwise [15, 16]).

2.4 Open-circuit voltage

The OCV is an important quantity characterizing batteries and electrochemical cells,[1] but it has no simple universal definition. Generally, it is the voltage measured by a potentiometer when no flux is passing through

---

[1] The OCV generally refers to a complete cell, while the term open-circuit potential (OCP) is used when referring to a half-cell measurement (against a reference).

the cell. This definition can be ambiguous, since the state of the cell is not specified. Perhaps the theoretically most appealing definition is that the electrochemical cell has been left undisturbed for a sufficiently long time to reach thermodynamic equilibrium. Such equilibrium would be characterized by minimization of Gibbs free energy of all possible electrochemical reactions taking place in the cell; see [8].

However, when measuring the OCV in practice, the cell is typically not allowed to relax to the complete equilibrium. The reason is twofold: (i) it would take unrealistically long and (ii) parasitic processes (like corrosion or crossover effects) would take place. The OCV is rather measured as the voltage once a plateau appears on the voltage vs. time plot. Therefore, it is necessary to consider the fastest processes affecting the practical OCV in the theoretical calculation, so that the measured plateau corresponds to equilibrium of these processes.

The OCV will then be defined as the difference in electric potential of electrons (proportional to the respective electrochemical potentials) at the positive and negative electrodes,

$$E = \Phi^P - \Phi^N. \tag{8}$$

Using the equilibrium of electrochemical reactions (4) and transport through the membrane (6), the OCV can be calculated as a function of activities of relevant species in the cell.

The OCV dependence on activities of the species can be turned to a dependence on molalities or concentrations of the species once activity coefficients are specified. Usually, however, data for activity coefficients are lacking, which leads to simplifying assumptions of ideal mixtures (activity coefficients equal to unity). This simplification results in inaccuracies as noted in [7]. In the case of water, however, one has to be a little more careful and use the Gibbs–Duhem equation, relating the derivative of the chemical potential of water to derivatives of chemical potentials of the other species. This is how water activity is expressed in terms of molalities of the other species; see [7] for more details.

To further express the OCV as a function of the state of charge[2] (SOC), it is first necessary to calculate molalities (or concentrations) of the species in the cell as functions of the SOC. One thus has to choose a concrete reaction pathway and to calculate the relation between the charge passing through the membrane and the changes of molalities of all relevant species in both electrolytes.

Let us now demonstrate this thermodynamic derivation of the formula describing the OCV on several examples.

3 Examples

We shall commence with a simple Ag/AgCl electrode connected with a standard hydrogen electrode. In this simple case both calculations of the Nernst equation coincide, and we discuss it for pedagogical clarity. Then we consider a zinc-air battery, where the thermodynamic approach overcomes the deficiencies of the formulae present in literature. Finally, the advantages of the thermodynamic approach are demonstrated on vanadium redox flow batteries, showing how the formula for OCV depends on the choice of the membrane (and the species transported through it).

3.1 A simple example: the silver-silver chloride electrode

Let us first recall the simple case of an Ag/AgCl cell with a standard hydrogen electrode (SHE). The positive electrode material is Ag coated with a thin film of porous AgCl, the main solute in the electrolyte is HCl, and we assume that an ideal hydrogen electrode serves as a negative electrode. Moreover, we assume that a perfectly permselective cation-exchange membrane, which only allows proton transfer, divides the positive

---

2 The SOC is equal to 1 in a fully charged state while being equal to 0 in a completely discharged state.

and negative compartments, and that the electrolyte is well stirred in each compartment. The reactions taking place on the positive half-cell are

$$Ag + Cl^- \rightleftharpoons AgCl + e^- \tag{9a}$$

and

$$AgCl \rightleftharpoons Ag^+ + Cl^-, \tag{9b}$$

while on the negative side we have

$$H^+ + e^- \rightleftharpoons \frac{1}{2}H_2. \tag{9c}$$

During discharge, electrons move from the anode (negative) through the external circuit to the cathode (positive), where they take part in the reduction reaction. Similarly, the hydrogen cations must be transferred from the anode, where they are formed, to the cathode through the electrolyte and membrane.

Assuming that the cell is in a steady state and that no current is passing through the external circuit (open-circuit condition), the electrochemical reactions do not proceed (have zero electrochemical affinities) and there is no ionic transport through the electrolyte or the membrane (zero gradient of electrochemical potential). Equilibrium in the positive electrode, P, reads

$$0 = \mu_{AgCl}^P + \tilde{\mu}_{e^-}^P - \mu_{Ag}^P - \tilde{\mu}_{Cl^-}^P. \tag{10}$$

This relation can be expanded using (1) and (2). The chemical potential of solids is typically near the standard value, and since the standard chemical potential of elements is zero, the chemical potential of silver is approximately zero, $\mu_{Ag}^P \approx 0$ (see Appendix A) near the standard temperature and pressure. Similarly, assuming the solution is saturated with AgCl, we can deduce $\mu_{AgCl}^P \approx \mu_{AgCl}^\circ$. The resulting positive half-cell potential is

$$\begin{aligned}\Phi^P &= \frac{1}{F}\left(\mu_{AgCl}^P - \mu_{Ag}^P - \tilde{\mu}_{Cl^-}^P\right) \\ &= \frac{1}{F}\left(\mu_{AgCl}^\circ - \mu_{Cl^-}^\circ - RT\ln a_{Cl^-}^P + F\varphi^P\right).\end{aligned} \tag{11}$$

Electrochemical equilibrium in the negative electrode, N, is expressed by

$$0 = \frac{1}{2}\mu_{H_2}^N - \tilde{\mu}_{H^+}^N - \tilde{\mu}_{e^-}^N, \tag{12a}$$

which can be rewritten as

$$\Phi^N = -\frac{1}{F}\left(\frac{1}{2}\mu_{H_2}^N - \tilde{\mu}_{H^+}^N\right) = -\frac{1}{F}\left(RT\ln\sqrt{a_{H_2}^N} - RT\ln a_{H^+}^N - F\varphi^N\right), \tag{12b}$$

where split (1) was employed as well as the convention that the standard chemical potential of hydrogen ions is zero (in aqueous solution), $\mu_{H^+}^\circ = 0$, and $\mu_{H_2}^\circ = 0$.

Finally, assuming that H$^+$ is the only species transported between the compartments (ideal cation-exchange membrane), equilibrium of transport through the membrane is expressed by

$$\tilde{\mu}_{H^+}^P = \tilde{\mu}_{H^+}^N. \tag{13}$$

The voltage measured by a potentiometer is given by

$$E = \Phi^P - \Phi^N = \underbrace{\frac{1}{F}\left(\mu_{AgCl}^\circ - \mu_{Cl^-}^\circ\right)}_{=E^\circ} - \frac{RT}{F}\ln\left(\frac{a_{Cl^-}^P a_{H^+}^N}{\sqrt{a_{H_2}^N}}\right) + \left(\varphi^P - \varphi^N\right). \tag{14}$$

The first term on the right hand side represents the standard potential and will be evaluated using thermodynamic data from Appendix A. The second term represents the contribution of the activities of the species. The third term, on the other hand, still has to be replaced by activities (and standard chemical potentials in the case of non-isothermal systems). To achieve that, the equilibrium of H^+ transport through the membrane (13) can be rewritten, using expansion (1), as

$$\varphi^P - \varphi^N = \frac{RT}{F} \ln \left(\frac{a_{H^+}^N}{a_{H^+}^P} \right).$$

(15)

Using this relation to simplify (14) leads to a formula describing the OCV of a AgCl cell connected with an SHE,

$$E = E^\circ - \frac{RT}{F} \ln \left(\frac{a_{Cl^-}^P \, a_{H^+}^P}{\sqrt{a_{H_2}^N}} \right).$$

(16)

Note that the above formula directly includes the membrane contribution, as all the necessary terms describing the system were already considered in (14). Furthermore, as the solution is saturated with AgCl, the formula does not depend on the activity of Ag^+, which remains constant. The assumption of saturation can of course be lifted (as discussed below on the example of corrosion), but we prefer keeping it here for simplicity.

The standard cell potential then becomes $E^\circ = \left(\mu_{AgCl}^\circ - \mu_{Cl^-}^\circ \right)/F = 0.223$ V. Assuming dilute electrolytes, the ionic activities can be approximated by their molalities,

$$a_{H^+}^P = \frac{b_{H^+}^P}{b^\circ} \qquad \text{and} \qquad a_{Cl^-}^P = \frac{b_{Cl^-}^P}{b^\circ}.$$

(17)

Finally, the activity of hydrogen can be approximated by the ratio of its partial pressure to the standard pressure, $a_{H_2}^N = p_{H_2}^N/p^\circ$. The formula for OCV then becomes

$$E = E^\circ - \frac{RT}{F} \ln \frac{b_{H^+}^P \, b_{Cl^-}^P}{(b^\circ)^2 \sqrt{\frac{p_{H_2}^N}{p^\circ}}},$$

(18)

which is compatible with the usual formula [17]. We have included this example to demonstrate the thermodynamic derivation of the OCV on the simple example where it coincides with the usual formula from the literature.

3.2 Zn-air redox flow battery

Different equations for the OCV appear in the Zn-air battery literature [18, 19, 20]. Although some authors do not explicitly present an OCV formula, they formulate the half-cell potentials and/or use them in the formulation of the Butler–Volmer equation. Here we show the correct thermodynamic derivation of the OCV formula for a zinc-air battery with an anion-exchange membrane [21, 22, 23, 24] and discuss some shortcomings of the equations found in the literature.

3.2.1 Electrochemical processes

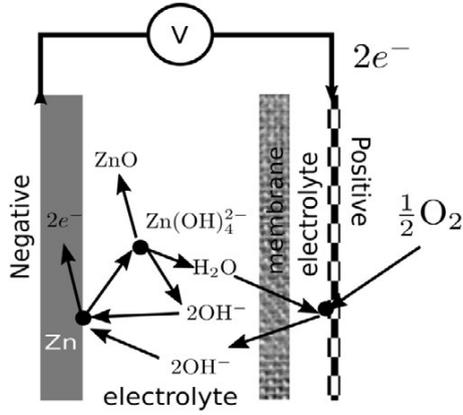The electrochemical reaction in the negative electrode of a zinc-air battery is

$$Zn + 4OH^- \rightleftharpoons Zn(OH)_4^{2-} + 2e^-,$$

(19a)
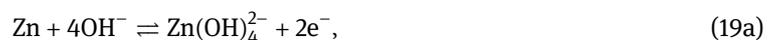
Figure 1: Simplified scheme of a zinc-air battery.

and is accompanied by the precipitation of zinc oxide,

$$\text{Zn(OH)}_4^{2-} \rightleftharpoons \text{ZnO} + 2\text{OH}^- + \text{H}_2\text{O}. \tag{19b}$$

On the positive half-cell, we have the following electrochemical reaction:

$$\frac{1}{2}\text{O}_2 + \text{H}_2\text{O} + 2e^- \rightleftharpoons 2\text{OH}^-. \tag{19c}$$

Note that water and hydroxide ions are produced on one side and consumed on the other. Assuming an ideal anion-exchange membrane, OH^- is the only ion transported through the membrane.

3.2.2 Equilibrium conditions

As in the previous example, we have to identify the equilibrium conditions at both electrodes and the membrane. Equilibrium of the negative electrode reaction is given by

$$0 = \tilde{\mu}_{\text{Zn}}^N + 4\tilde{\mu}_{\text{OH}^-}^N - \tilde{\mu}_{\text{Zn(OH)}_4^{2-}}^N - 2\tilde{\mu}_{e^-}^N, \tag{20}$$

which can be rewritten as

$$0 = \mu_{\text{Zn}}^\circ + 4\mu_{\text{OH}^-}^\circ + 4RT \ln a_{\text{OH}^-}^N - 4F\varphi^N - \mu_{\text{Zn(OH)}_4^{2-}}^\circ - RT \ln a_{\text{Zn(OH)}_4^{2-}}^N + 2F\varphi^N + 2F\Phi^N. \tag{21}$$

Analogically, equilibrium of the positive electrode half-reaction reads

$$\begin{aligned}
0 &= \frac{1}{2}\mu_{\text{O}_2}^P + \mu_{\text{H}_2\text{O}}^P + 2\tilde{\mu}_{e^-}^P - 2\tilde{\mu}_{\text{OH}^-}^P \\
&= \frac{1}{2}\mu_{\text{O}_2}^\circ + \frac{1}{2}RT \ln a_{\text{O}_2}^P + \mu_{\text{H}_2\text{O}}^\circ + RT \ln a_{\text{H}_2\text{O}}^P \\
&\quad -2F\Phi^P - 2\mu_{\text{OH}^-}^\circ - 2RT \ln a_{\text{OH}^-}^P + 2F\varphi^P.
\end{aligned} \tag{22}$$

Equilibrium of the membrane transport is expressed by

$$\tilde{\mu}_{\text{OH}^-}^N = \tilde{\mu}_{\text{OH}^-}^P. \tag{23}$$

3.2.3 Open-circuit voltage

Combining (21) and (22) the OCV of the battery is then given by

$$
E = \Phi^P - \Phi^N \tag{24}
$$
$$
= \frac{1}{2F} \left(\mu^\circ_{Zn} + 2\mu^\circ_{OH^-} - \mu^\circ_{Zn(OH)_4^{2-}} + \frac{1}{2}\mu^\circ_{O_2} + \mu^\circ_{H_2O} \right)
$$
$$
+ \frac{RT}{2F} \ln \left(\frac{\sqrt{a^P_{O_2}} \, a^P_{H_2O} (a^N_{OH^-})^4}{(a^P_{OH^-})^2 a^N_{Zn(OH)_4^{2-}}} \right)
$$
$$
+ \varphi^P - \varphi^N. \tag{25}
$$

The term involving the electrolyte potentials can be substituted using the equilibrium of the transport of OH^- through the membrane (23) such that

$$
\varphi^P - \varphi^N = \frac{RT}{2F} \ln \left(\frac{a^P_{OH^-}}{a^N_{OH^-}} \right)^2. \tag{26}
$$

Plugging this relation back into eq. (24) gives the final form of the general formula for OCV,

$$
E = E^\circ + \frac{RT}{2F} \ln \left(\frac{\sqrt{a^P_{O_2}} \, a^P_{H_2O} (a^N_{OH^-})^2}{a^N_{Zn(OH)_4^{2-}}} \right), \tag{27}
$$

where

$$
E^\circ = \frac{1}{2F} \left(\mu^\circ_{Zn} + 2\mu^\circ_{OH^-} - \mu^\circ_{Zn(OH)_4^{2-}} + \frac{1}{2}\mu^\circ_{O_2} + \mu^\circ_{H_2O} \right) = 1.60 \text{ V}, \tag{28}
$$

using the standard chemical potential values compiled in Appendix A.

3.2.4 Comparison with the usual OCV

The most frequently used formula for OCV of Zn-air batteries in literature (e. g., [18]) is

$$
E_{usual} = E^P - E^N = E^\circ + \frac{RT}{2F} \ln \frac{\sqrt{a^P_{O_2}} \, a^P_{H_2O} (c^N_{OH^-})^4}{c^N_{Zn(OH)_4^{2-}} (c^P_{OH^-})^2}. \tag{29}
$$

Formula (27) differs from the usual formula (29) by the terms coming from the equilibrium of transport of OH^- through the membrane (26). These terms can be referred to as the membrane (or Donnan) potential. By including them, formula (27) becomes more precise than the usual formula. Therefore, it is important to go back to the thermodynamic roots of the Nernst equation in the case of zinc-air batteries.

However, note that when using a porous separator in the battery instead of the ion-exchange membrane, practically any species small enough to pass through the pores can be transported between positive and negative compartments. To obtain a relation for $\varphi^P - \varphi^N$ one has to determine the electrochemical process that equilibrates first across the separator. For instance, a different charged species can be the first to equilibrate, and eq. (23) has to be replaced by the analogical equilibrium equation for the species. In some situations, one can also assume that the electrolyte is perfectly mixed in the whole system, which, using (7), leads to

$$
\varphi^P - \varphi^N = 0. \tag{30}
$$

Even though most modeling works on Zn-air systems study cells with porous separators instead of membranes, several of the formulae present in the literature [18, 19, 20] have deficiencies that would have been

prevented using the thermodynamic derivation described here. For example, [20] presents a formula where the activity term has an opposite sign. In [18], the concentrations of O_2 and H_2O are used instead of their activities. For pure liquids (or in this case solvents) and dissolved gases the relation between activities and concentrations requires a different approach to the reference concentration. The proper approach for the dissolved gas concentration was identified in [19], where the reference state at standard conditions is given by Henry's law.

Moreover, most recent works [25, 19, 20] also rely on incorrect values for the standard potential of the zinc electrode. The value used, $E_{Zn}^{0,*} = -1.286$ V (vs. SHE), is the one presented in [26, 27], which is based on the Gibbs energy of formation of $Zn(OH)_4^{2-}$ reported by [28]. Nonetheless, the measurements carried out in [28] have been criticized by several reviews [29, 30, 31] due to inadequate pH measurements. In this work, we used the value of $\Delta_f G_{Zn(OH)_4^{2-}}^\circ$ recommended by [31], which is compatible with the ones presented in [29] and [32], leading to $E_{Zn}^0 = -1.20$ V (vs. SHE), which is in good agreement with the experimental potentiometric measurements reported by [33, 34]. The use of an inaccurate standard potential leads to errors in the assessment of the OCV and the kinetic constants for the zinc reaction. Using the proper thermodynamic derivation of the Nernst equation presented here would help to critically assess the standard potentials by identifying the individual compounds for which the values of $\Delta_f G^\circ$ are not well stabilized (in this case $Zn(OH)_4^{2-}$).

3.2.5 Half-cell potential of the zinc electrode

In the absence of available data in the literature for the potential of a zinc-air battery as a function of species concentration, we compare our thermodynamic derivation with the experimental data and the Nernst equation presented in [20] for a zinc electrode against an Hg/HgO reference. To compare the data, we first derive the half-cell potential of the zinc electrode with an Hg/HgO reference.

Commonly, reference electrodes are calibrated against the SHE. For the Hg/HgO reference electrode with 1 M KOH used in [20] the potential against SHE as reported by the same authors is

$$E_{Hg/HgO}^{SHE} = \Phi^{Hg/HgO} - \Phi^{SHE} = 0.1157 \text{ V}. \tag{31}$$

Such measured value already includes the effects of activity terms and junction potentials. This value can be used to determine the OCP of a zinc electrode against the aforementioned Hg/HgO reference. The OCP of the zinc electrode against a hypothetical SHE can be determined from eqs. (12b) and (20). Using the definition of SHE and the assumption of unit activities for solid species (i. e., $a_{H_2}^{SHE} = a_{H^+}^{SHE} = a_{Zn} = 1$) leads to

$$E_{Zn}^{SHE} = \Phi^{Zn} - \Phi^{SHE} = E_{Zn}^\circ - \frac{RT}{2F} \ln\left(\frac{(a_{OH^-}^{Zn})^4}{a_{Zn(OH)_4^{2-}}^{Zn}}\right) + (\varphi^{Zn} - \varphi^{SHE}). \tag{32}$$

Therefore, using (31) and (32), we can construct the theoretical potential of a zinc electrode with an Hg/HgO reference. By assuming a negligible difference in Maxwell potentials ($\varphi^{Zn} - \varphi^{SHE} \approx 0$), it results in

$$E_{Zn}^{Hg/HgO} = \Phi^{Zn} - \Phi^{Hg/HgO} = (E_{Zn}^\circ - E_{Hg/HgO}^{SHE}) - \frac{RT}{2F} \ln\left(\frac{(a_{OH^-}^{Zn})^4}{a_{Zn(OH)_4^{2-}}^{Zn}}\right). \tag{33}$$

In Figure 2, it can be seen that the simplified approach to the Nernst equation led to discrepancies between the formula and experiment. Conversely, when using the thermodynamic derivation of the Nernst equation with the proper value of E_{Zn}^0, the theoretical curve provides a better description of the experimental data.

3.2.6 Effect of mixed potentials

The reaction scheme (19a) and (19c) does not take into account side reactions happening on the electrodes. In reality, at the equilibrium potential of the zinc electrode the hydrogen evolution reaction (HER) can also
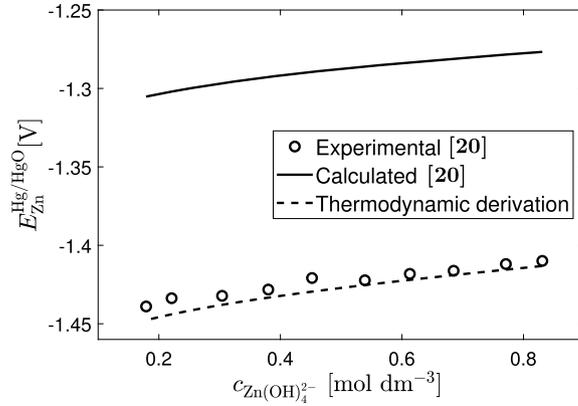
Figure 2: Comparison of the thermodynamic derivation of the Nernst equation (33) with the experimental and calculated data shown by [20].

take place:

$$2H_2O + 2e^- \rightleftharpoons H_2 + 2OH^-. \tag{34}$$

This is a corrosion process that consumes active material (zinc) and shifts the OCV of the system. The half-cell potential in this situation is usually referred to as the mixed potential. Therefore, this case must be assessed in terms of non-equilibrium thermodynamics as the system is no longer in equilibrium.[3]

The fast equilibrium of the corrosion pair (19a) and (34) is characterized by equality of their currents (no net current). Reaction rates are usually expressed by the Butler–Volmer equation

$$j = j_0 \left(e^{\alpha \tilde{A}/RT} - e^{-(1-\alpha)\tilde{A}/RT} \right); \tag{35}$$

see, e. g., [7] for a thermodynamic origin of this equation (based on the concept of possibly asymmetric dissipation potentials) or [17] for a kinetic origin. The charge transfer coefficient α describes whether the transition state is closer to the oxidized or reduced species; typically it is assumed to be equal to 1/2 [17]. The exchange current j_0 prefactor can be either constant or dependent on concentrations of the reactants and products (cf. [35] or [5] for the Boltzmann equation), and it is positive in the direction of oxidation.

In general, the mixed potential can be determined by numerical methods calculating the potential at which the sum of currents for the anodic and cathodic reactions in the electrode (in this case zinc dissolution and hydrogen evolution, respectively) is zero. Nonetheless, under certain conditions the Butler–Volmer equation can be simplified, thus leading to analytical solutions of the mixed potential. In the case of high $|\tilde{A}|$, the Butler–Volmer equation (35) reduces to the Tafel equation

$$j = j_0 e^{(1-\alpha)\tilde{A}/RT}, \tag{36}$$

while for the low $|\tilde{A}|$ case it turns to a linear relation,

$$j = j_0 \frac{\tilde{A}}{RT}, \tag{37}$$

between the current and the overpotential. Note that the charge transfer coefficient α disappears in the low-current limit.

---

3 Note that there is also a mixed potential in the air electrode, which leads to another shift of the OCV. Such case can also be treated in terms of non-equilibrium thermodynamics but, due to its sluggish kinetics, it is difficult to assess as it will be heavily dependent on the catalyst and support as well as the presence of impurities (even just traces [35]).

The most common case presented in the corrosion literature [36, 37] is that in which both reactions are in the Tafel regime (high $|\tilde{\mathcal{A}}|$). However, such regime does not apply for the case of zinc battery electrodes (which contain corrosion inhibitors) as they are reported to have fast kinetics and relatively high hydrogen overpotentials [38, 39, 40]. Consequently, in zinc-based battery systems under OCV conditions the HER is usually in the Tafel regime while the zinc dissolution is in the linear regime. The numerical derivation of such example is discussed in Appendix B.

3.3 All-vanadium flow cell

The vanadium redox flow battery (VRFB) has been analyzed in [7] and [41]. Let us briefly recall the calculation in a condensed form and show how it differs from the usual formula from [42],

$$E_{usual}^{*} = E^{\circ} + \frac{RT}{F} \ln \frac{c_{VO_2^+}^P c_{V^{2+}}^N \left(c_{H^+}^P\right)^2}{c_{VO^{2+}}^P c_{V^{3+}}^N}. \tag{38}$$

We shall consider two cases: a VRFB with a cation-exchange (catex) membrane and a VRFB with an anion-exchange (anex) membrane. The OCV formula will be different in the two cases.

The main electrochemical reactions taking place in VRFBs can be summarized as

$$VO_2^+ + e^- + 2H^+ \rightleftharpoons VO^{2+} + H_2O \tag{39a}$$

on the positive side and

$$V^{2+} \rightleftharpoons V^{3+} + e^- \tag{39b}$$

on the negative side. Furthermore, we should also consider ionic transport through the membrane, H^+ in the catex case and HSO_4^- in the anex case. Let us now discuss these two cases separately.

3.3.1 Cation-exchange membrane

The equations expressing equilibrium of the electrochemical reactions are

$$\tilde{\mu}_{VO_2^+}^P - F\Phi^P + 2\tilde{\mu}_{H^+}^P = \tilde{\mu}_{VO^{2+}}^P + \mu_{H_2O}^P \tag{40a}$$

and

$$\tilde{\mu}_{V^{2+}}^N = \tilde{\mu}_{V^{3+}}^N - F\Phi^N. \tag{40b}$$

Equilibrium of the ionic transport through the membrane means that

$$\tilde{\mu}_{H^+}^N = \tilde{\mu}_{H^+}^P, \tag{41}$$

which can be rewritten as

$$\varphi^P - \varphi^N = \frac{RT}{F} \ln \frac{a_{H^+}^N}{a_{H^+}^P}, \tag{42}$$

where $\varphi^{P,N}$ are the Maxwell potentials in the positive and negative electrolytes, respectively.

The OCV can then be expressed as

$$\begin{aligned} E = \Phi^P - \Phi^N &= \frac{1}{F}\left(\tilde{\mu}_{VO_2^+}^P + 2\tilde{\mu}_{H^+}^P - \tilde{\mu}_{VO^{2+}}^P - \mu_{H_2O}^P\right) + \frac{1}{F}\left(\tilde{\mu}_{V^{2+}}^N - \tilde{\mu}_{V^{3+}}^N\right) \\ &= \frac{1}{F}\left(\mu_{VO_2^+}^{\circ} - \mu_{VO^{2+}}^{\circ} - \mu_{H_2O}^{\circ} + \mu_{V^{2+}}^{\circ} - \mu_{V^{3+}}^{\circ}\right) \\ &\quad + \frac{RT}{F} \ln \frac{a_{VO_2^+}^P (a_{H^+}^P)^2 a_{V^{2+}}^N}{a_{VO^{2+}}^P a_{H_2O}^P a_{V^{3+}}^N} \\ &\quad + \varphi^P - \varphi^N, \end{aligned} \tag{43}$$

where split (1) was used. Note the last line, where the difference in Maxwell electrostatic potentials remains. This arises from the form of eqs. (39), where the charge on the left hand sides is equal to the charge on the right hand sides, but is not zero. To get rid of the Maxwell potential difference, the membrane equilibrium equation (42) must be used, which leads to

$$E = E^\circ + \frac{RT}{F} \ln \frac{a_{VO_2^+}^P a_{V^{2+}}^N a_{H^+}^P a_{H^+}^N}{a_{VO^{2+}}^P a_{H_2O}^P a_{V^{3+}}^N}, \tag{44}$$

where the standard cell potential is

$$E^\circ = \frac{1}{F} \left(\mu_{VO_2^+}^\circ - \mu_{VO^{2+}}^\circ - \mu_{H_2O}^\circ + \mu_{V^{2+}}^\circ - \mu_{V^{3+}}^\circ \right) = 1.256\,\text{V}, \tag{45}$$

taking values of the standard Gibbs energies of formation from Appendix A. Formula (44) is the formula for the OCV in the catex case. To compare it with experimental data, which are usually expressed in terms of SOC, the activities have to be expressed in terms of molalities.

3.3.2 Anion-exchange membrane

We shall now discuss VRFBs with anex membranes through which HSO_4^- ions are transported. The equilibrium equations (40) are the same as in the anex case. The difference is in the ion transport as eq. (42) changes to

$$\tilde{\mu}_{HSO_4^-}^N = \tilde{\mu}_{HSO_4^-}^P, \tag{46}$$

which can be rewritten as

$$\varphi^P - \varphi^N = \frac{RT}{F} \ln \frac{a_{HSO_4^-}^P}{a_{HSO_4^-}^N}. \tag{47}$$

The OCV (43) then turns to

$$E = E^\circ + \frac{RT}{F} \ln \frac{a_{VO_2^+}^P a_{V^{2+}}^N (a_{H^+}^P)^2 a_{HSO_4^-}^P}{a_{VO^{2+}}^P a_{H_2O}^P a_{V^{3+}}^N a_{HSO_4^-}^N}. \tag{48}$$

Again, to accurately compare it with the experimental dependence of the OCV on the SOC, one needs to express the activities, exploiting, e. g., [43], in terms of molalities. Assuming unity activity coefficients, the comparison is shown in Figure 3, where the data are taken from [7].

Note, in particular, that the formulae for OCV are different in the anex and catex cases. Such difference cannot be seen in the simplified construction of the Nernst equation.

The thermodynamic formula for the OCV is different from the usual one available in the literature [42, 6]. Moreover, the formula for OCV depends on the choice of the membrane, more precisely on the species that is transported through the membrane [7]. Although the electrochemical equations are the same, the equilibrium equation for transport through the membrane is different, as well as the resulting Nernst equation.

3.4 Other systems

As highlighted in the previous section, the thermodynamic derivation of the Nernst equation is particularly important in systems where either cation-exchange or anion-exchange membranes can be used, such as VRFBs or iron-chromium (Fe/Cr) redox flow batteries [44, 45, 46]. Recently, organic redox flow battery systems, such as the quinone/hydroquinone couple, have also being tested with both catex and anex membranes
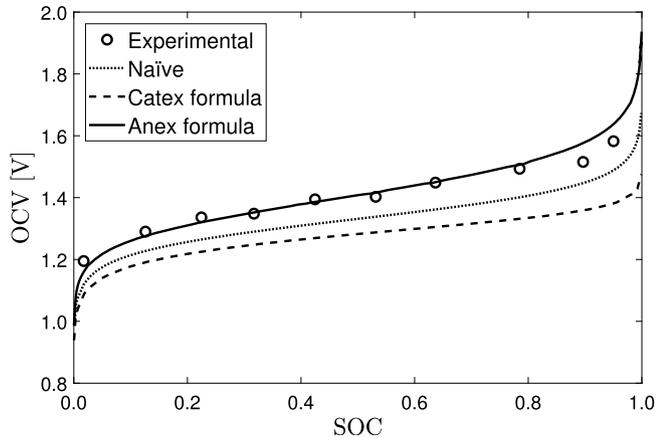
Figure 3: Comparison of the naïve formula (38) and catex and anex formulae ((44) and (48), respectively) with experimental data for an anex membrane (data re-used from [7]). The naïve and catex formulae which are close to the usual Nernst equation for VRFBs are clearly deficient. For comparison of the formula for catex membranes with experimental data, see [7].

[47, 48, 49]. Furthermore, in VRFB systems, this is relevant not only for single cells but also for stacks. For example, the thermodynamic derivation must be considered for VRFB stacks using cells alternating catex and anex membranes, which have been proposed as a solution to compensate the capacity fade of VRFBs due to electroosmosis [50].

Finally, current development of redox flow batteries is also considering systems with three electrolyte compartments which combine both anion-exchange and cation-exchange membranes in the same device [51, 52]. For example, in the zinc-iron system presented by [52] the negative and middle electrolytes are separated by a catex membrane (transporting Na^+ ions) while the positive and middle electrolytes are separated by an anex membrane (transporting Cl^- ions). The thermodynamic Nernst equation will also have to be considered when describing such systems as different species are transported between the compartments.

4 Conclusions

The simplified way towards the Nernst equation is extensively used in the literature. Nonetheless, it can lead to inaccurate conclusions when analyzing and modeling battery systems, for instance in zinc-air and vanadium redox flow batteries. The thermodynamic back-to-the-roots derivation of the Nernst equation starting from non-equilibrium thermodynamics provides a more robust way towards the OCV which takes into account all the necessary interfaces and possible non-equilibrium phenomena. In particular, in systems with ion-exchange membranes the OCV depends on the species transported through the membrane. In vanadium redox flow batteries, where both anion-exchange and cation-exchange membranes can be used, two different forms of the Nernst equation are obtained. Since the state at which the OCV is measured is not the thermodynamic equilibrium, non-equilibrium processes like corrosion can contribute to the value of the OCV. In summary, non-equilibrium thermodynamics should be considered when determining the Nernst equation.

Appendix A. Gibbs energies of formation

The standard chemical potentials can be taken as equal to the standard Gibbs energies of formation $\Delta_f G^\circ$ [17, 32]. The standard Gibbs energy of formation of elements is zero by definition, as well as $\Delta_f G^\circ$ of H^+ in water. Table 1 shows the standard Gibbs energy of formation of the chemical compounds used in this paper following [32] (except where indicated otherwise). The reference state corresponds to a temperature of 298.15 K, a pressure of 1 bar, and a molality of $1\,\text{mol}\,\text{kg}^{-1}$.

Table 1: Standard Gibbs energies of formation. Phases: solid (s), liquid (l), and aqueous solution (aq).

Compound	Phase	$\Delta_f G^\circ$ [kJ mol^{-1}]
H^+	aq	0
Cl^-	aq	−131.288
AgCl	s	−109.789
OH^-	aq	−157.244
H_2O	l	−237.129
$Zn(OH)_4^{2-}$	aq	−860 [53]
V^{2+}	aq	−217.6
V^{3+}	aq	−242.3
VO^{2+}	aq	−446.4 [54]
VO_2^+	aq	−587.0 [54]

Appendix B. Corrosion on zinc electrodes

As noted in the main text, the HER corresponds with the Tafel regime for zinc systems under OCV conditions (using the typical value $\alpha = 1/2$) and the zinc dissolution is in the linear regime, that is,

$$j^{\text{HER}} = -j_0^{\text{HER}} e^{\tilde{A}_{\text{HER}}/(2RT)}, \tag{49a}$$

$$j^{\text{Zn}} = j_0^{\text{Zn}} \tilde{A}_{\text{Zn}}/(RT), \tag{49b}$$

for reactions (34) and (19a), respectively. The electrochemical affinities are defined as

$$\tilde{A}_{\text{HER}} = 2\mu_{\text{H}_2\text{O}} - 2F\Phi^N - \mu_{\text{H}_2} - 2\tilde{\mu}_{\text{OH}^-}^N, \tag{50a}$$

$$\tilde{A}_{\text{Zn}} = \mu_{\text{Zn}}^N + 4\tilde{\mu}_{\text{OH}^-}^N - \tilde{\mu}_{\text{Zn(OH)}_4^{2-}}^N + 2F\Phi^N. \tag{50b}$$

The mixed potential equilibrium corresponds, assuming the same electroactive area for both reactions, to an equality of currents,

$$j^{\text{corr}} = j^{\text{Zn}} = -j^{\text{HER}}, \tag{51}$$

which can be rewritten as a non-linear algebraic equation for $\Phi^N - \varphi^N$,

$$\frac{1}{RT}\left(\mu_{\text{Zn}}^N + 4\mu_{\text{OH}^-}^N - \mu_{\text{Zn(OH)}_4^{2-}}^N + 2F(\Phi^N - \varphi^N)\right) = \frac{j_0^{\text{HER}}}{j_0^{\text{Zn}}} e^{\left(\frac{2\mu_{\text{H}_2\text{O}}^N - \mu_{\text{H}_2}^N - 2\mu_{\text{OH}^-}^N}{2RT}\right)} e^{-\frac{F}{RT}(\Phi^N - \varphi^N)}. \tag{52}$$

Introducing the dimensionless quantities $\hat{A}_{\text{Zn}} = \dfrac{\mu_{\text{Zn}}^N + 4\mu_{\text{OH}^-}^N - \mu_{\text{Zn(OH)}_4^{2-}}^N}{RT}$, $\hat{A}_{\text{HER}} = \dfrac{2\mu_{\text{H}_2\text{O}}^N - \mu_{\text{H}_2}^N - 2\mu_{\text{OH}^-}^N}{2RT}$, $\hat{j}_0 = \dfrac{j_0^{\text{HER}}}{j_0^{\text{Zn}}}$, and $\hat{\Phi} = (\Phi^N - \varphi^N)\dfrac{F}{RT}$ results in the non-dimensional equation

$$\hat{\Phi} = -\frac{1}{2}\hat{A}_{\text{Zn}} + j_0 e^{\hat{A}_{\text{HER}}} e^{-\hat{\Phi}}. \tag{53}$$

This non-dimensional non-linear algebraic equation can be solved by the Banach fixed point iteration (proof of convergence can be found in C), using $\hat{\Phi}^{(n)} = T(\hat{\Phi}^{(n-1)})$ with mapping $T(\hat{\Phi})$ defined as the right hand side of eq. (53). Taking the zeroth approximation $\hat{\Phi}^0 = \hat{A}_{Zn}$, which corresponds to the equilibrium potential of the zinc reaction, the first approximation reads

$$\hat{\Phi}^{(1)} = -\frac{1}{2}\hat{A}_{Zn} + j_0 e^{\hat{A}_{HER}} e^{-\hat{A}_{Zn}}, \tag{54a}$$

while

$$\hat{\Phi}^{(i)} = -\frac{1}{2}\hat{A}_{Zn} + j_0 e^{\hat{A}_{HER}} e^{-\hat{\Phi}^{(i-1)}}. \tag{54b}$$

Let us denote the final solution as $\hat{\Phi}^N$.

The formula for OCV is defined as the difference of electrochemical potentials of electrons as before,

$$\begin{aligned} E = \Phi^P - \Phi^N &= \frac{1}{2F}\left(\frac{1}{2}\mu_{O_2}^P + \mu_{H_2O}^P - 2\tilde{\mu}_{OH^-}^P\right) \\ &\quad -\frac{RT}{F}\hat{\Phi}^N - \varphi^N \\ &= \frac{1}{2F}\left(\frac{1}{2}\mu_{O_2}^P + \mu_{H_2O}^P - 2\mu_{OH^-}^P - 2RT\hat{\Phi}^N\right) \\ &\quad +\varphi^P - \varphi^N, \end{aligned} \tag{55}$$

where $\hat{\Phi}$ is the result of the fixed point iteration. Note that the last expression consists of a chemical contribution and an electrical contribution, which is to be replaced by a transport equilibrium condition, e. g., formula (23).

Let us assume a Zn electrode immersed in a perfectly mixed solution of 6 M KOH in a system at 25 °C with a low hydrogen pressure ($p_{H_2}/p° = 10^{-6}$). We will simplify the calculations by assuming that the H_2 bubbles are immediately washed out from the electrode (due to the strong mixing) and that the rest of the species have unit activities (i. e., $a_{Zn(OH)_4^{2-}} = a_{H_2O} = 1$). The negative half-cell potential ϕ^N resulting from the fixed point iteration for different values of $\hat{j_0}$ is shown in Table 2. Note that the value of $\hat{j_0}$ changes with the use of additives in the zinc electrode or the electrolyte [55, 56].

Table 2: Mixed potential for a Zn electrode with H_2 evolution and number of iterations as a function of $\hat{j_0}$.

$\hat{j_0}$	ϕ^N	Nr. of iterations
10^{-3}	−1.261	12
10^{-4}	−1.278	2
10^{-5}	−1.281	1
10^{-6}	−1.282	0

Appendix C. Banach fixed point theorem

Having a Banach space X (e. g., real numbers with a metric given the absolute value) and a contraction mapping $T : X \rightarrow X$ satisfying

$$\exists q \in (0,1) \quad \text{for which} \quad |T(x) - T(y)| \leq q \cdot |x - y| \quad \forall x, y \in X, \tag{56}$$

there is only one fixed point of the mapping, $T(\bar{x}) = \bar{x}$, and it is the limit of iterations $x^{(n)} = T(x^{(n-1)})$. This is the Banach contraction theorem [57].

In order to apply it to eq. (53), we have to verify that the mapping

$$T(\hat{\Phi}) = -\frac{1}{2}\hat{A}_{Zn} + j_0 e^{\hat{A}_{HER}} e^{-\hat{\Phi}} \tag{57}$$

is really a contraction. Therefore, we calculate (assuming $\hat{\Phi}_1 \geq \hat{\Phi}_2$ without any loss of generality)

$$|T(\hat{\Phi}_1) - T(\hat{\Phi})_2| = j_0 e^{\hat{A}_{HER}} \left| e^{-\hat{\Phi}_1} - e^{-\hat{\Phi}_2} \right| \tag{58}$$

$$= j_0 e^{\hat{A}_{HER}} \left| \int_{\hat{\Phi}_2}^{\hat{\Phi}_1} -e^{-\hat{\Phi}} d\hat{\Phi} \right|$$

$$\leq j_0 e^{\hat{A}_{HER}} \int_{\hat{\Phi}_0 - \epsilon}^{\hat{\Phi}_0 + \epsilon} e^{-\hat{\Phi}} d\hat{\Phi} = j_0 e^{\hat{A}_{HER}} \cdot 2 e^{-\hat{\Phi}_0} \sinh(\epsilon),$$

where it was assumed that $\hat{\Phi}_0$ is in the vicinity of a value $\hat{\Phi}_0$, $\hat{\Phi} \in (\hat{\Phi}_0 - \epsilon, \hat{\Phi}_0 + \epsilon)$. If $j_0 e^{\hat{A}_{HER}}$ is low enough, then the mapping is indeed a contraction, i. e., $|T(\hat{\Phi}_1) - T(\hat{\Phi})_2| \leq q$ for some $q < 1$. This is usually satisfied because of the small value of j_0 given by the small value of j_0^{HER}, and the iteration then converges.

References

[1] Maria Skyllas-Kazacos and Michael Kazacos, State of charge monitoring methods for vanadium redox flow battery control, *J. Power Sources* **196** (2011), no. 20, 8822–8827.

[2] Jianlu Zhang, Yanghua Tang, Chaojie Song, Jiujun Zhang and Haijiang Wang, PEM fuel cell open circuit voltage (OCV) in the temperature range of 23 °C to 120 °C, *Journal of Power Sources* **163** (2006), no. 1 SPEC. ISS., 532–537.

[3] W. Nernst and H. T. Tizard, *Theoretical Chemistry from the Standpoint of Avogadro's Rule & Thermodynamics*, Macmillan and Company, Ltd., 1916.

[4] L. D. Landau and E. M. Lifschitz, *Statistical Physics*, Number pt. 1 in Course of Theoretical Physics, Pergamon Press, 1969.

[5] Michal Pavelka, Václav Klika and Miroslav Grmela, *Multiscale Thermo-Dynamics*, de Gruyter, Berlin, 2018.

[6] K. W. Knehr and E. C. Kumbur, Open circuit voltage of vanadium redox flow batteries: Discrepancy between models and experiments, *Electrochem. Commun.* **13** (Apr. 2011), no. 4, 342–345.

[7] Michal Pavelka, Petr Mazur and Frank Wandschneider, Thermodynamic derivation of open circuit voltage in vanadium redox flow batteries, *J. Power Sources* (2015). Submitted.

[8] Petr Vágner, Roman Kodým and Karel Bouzek, Thermodynamic analysis of high temperature steam and carbon dioxide systems in solid oxide cells, *Sustain. Energy Fuels* **3** (2019), 2076–2086.

[9] I. N. Levine, *Physical Chemistry*, McGraw-Hill, 2008.

[10] S. Kjelstrup and D. Bedeaux, *Non-Equilibrium Thermodynamics of Heterogeneous Systems*, Series on Advances in Statistical Mechanics, World Scientific, 2008.

[11] Michal Pavelka, Václav Klika, Petr Vágner and František Maršík, Generalization of exergy analysis, *Appl. Energy* **137** (2015), no. 0, 158–172.

[12] Wolfgang Dreyer, Clemens Guhlke and Rüdiger Müller, A new perspective on the electron transfer: recovering the Butler-Volmer equation in non-equilibrium thermodynamics, *Phys. Chem. Chem. Phys.* **18** (2016), 24966–24983.

[13] E. A. Guggenheim, *Thermodynamics: An Advanced Treatment for Chemists and Physicists*, Monographs on Theoretical and Applied Physics, North-Holland Pub. Co., 1949.

[14] S. R. de Groot and P. Mazur, *Non-Equilibrium Thermodynamics*, Dover Publications, New York, 1984.

[15] J. Fuhrmann, C. Guhlke, A. Linke, C. Merdon and R. Müller, Induced charge electroosmotic flow with finite ion size and solvation effects, *Electrochim. Acta* **317** (2019), 778–785.

[16] Petr Vágner, Clemens Guhlke, Vojtěch Miloš, Rüdiger Müller and Jürgen Fuhrmann, A continuum model for yttria-stabilized zirconia incorporating triple phase boundary, lattice structure and immobile oxide ions, *J. Solid State Electrochem.* **23** (2019), no. 10, 2907–2926.

[17] P. W. Atkins and J. De Paula, *Atkins' Physical Chemistry*, Oxford University Press, 2002.

[18] Daniel Schröder and Ulrike Krewer, Model based quantification of air-composition impact on secondary zinc air batteries, *Electrochim. Acta* **117** (2014), 541–553.

[19] Johannes Stamm, Alberto Varzi, Arnulf Latz and Birger Horstmann, Modeling nucleation and growth of zinc oxide during discharge of primary zinc-air batteries, *J. Power Sources* **360** (2017), 136–149.

[20] Christian Zelger, Michael Süssenbacher, Andreas Laskos and Bernhard Gollas, State of charge indicators for alkaline zinc-air redox flow batteries, *J. Power Sources* **424** (2019), 76–81.

[21] Ali Abbasi, Soraya Hosseini, Anongnat Somwangthanaroj, Ahmad Azmin Mohamad and Soorathep Kheawhom. Poly(2,6-dimethyl-1,4-phenylene oxide)-based hydroxide exchange separator membranes for zinc–air battery, *Int. J. Mol. Sci.* **20** (2019), no. 15, 3678.

[22] Dewi Eniya Listiani, Kenichi Oyaizu, Hiroyuki Nishide and Eishun Tsuchida. Cationic polysulfonium membrane as separator in zinc-air cell, *J. Power Sources* **115** (2003), no. 1, 149–152.

[23] Naoko Fujiwara, Masaru Yao, Zyun Siroma, Hiroshi Senoh, Tsutomu Ioroi and Kazuaki Yasuda, Reversible air electrodes integrated with an anion-exchange membrane for secondary air batteries, *J. Power Sources* **196** (2011), no. 2, 808–813.

[24] Misgina Tilahun Tsehaye, Fannie Alloin and Cristina Iojoiu, Prospects for anion-exchange membranes in alkali metal–air batteries, *Energies* **12** (2019), 24.

[25] Erich Deiss, F. Holzer and O. Haas, Modeling of an electrically rechargeable alkaline Zn-air battery, *Electrochim. Acta* **47** (2002), no. 25, 3995–4010.

[26] A. J. Bard, R. Parsons and J. Jordan, *Standard Potentials in Aqueous Solution*, Monographs in Electroanalytical Chemistry and Electrochemistry, Taylor & Francis, 1985.

[27] John Aurie Dean, *Lange's Handbook of Chemistry*, McGraw-Hill, Inc., New York, London, 1999.

[28] A. O. Gubeli and J. Ste-Marie, Stabilité des complexes hydroxo et produits de solubilité des hydroxydes de métaux. I. Argent et zinc, *Can. J. Chem.* **45** (1967), no. 8, 827–832.

[29] C. F. Baes and R. E. Mesmer, *The Hydrolysis of Cations*, Wiley, 1976.

[30] J. Powell Kipton, Paul L. Brown, Robert H. Byrne, Tamas Gajda, Glenn Hefter, Ann Kathrin Leuz, et al., Chemical speciation of environmentally significant metals with inorganic ligands. Part 5: The Zn^{2+} + OH^-, Cl^-, CO_3^{2-}, SO_4^{2-}, and PO_4^{3-} systems (IUPAC Technical Report), *Pure Appl. Chem.* **85** (2013), no. 12, 2249–2311.

[31] Yu Zhang and Mamoun Muhammed, Critical evaluation of thermodynamics of complex formation of metal ions in aqueous solutions, *Hydrometallurgy* **60** (May 2001), no. 3, 215–236.

[32] D. D. Wagman, W. H. Evans, V. B. Parker, R. H. Schumm, I. Halow, S. M. Bailey, et al., The NBS tables of chemical thermodynamic properties – selected values for inorganic and C-1 and C-2 organic substances in SI units, *J. Phys. Chem. Ref. Data* **11** (1982), no. 2, 1.

[33] D. P. Boden, R. B. Wylie and V. J. Spera, The electrode potential of zinc amalgam in alkaline zincate solutions, *J. Electrochem. Soc.* **118** (1971), no. 8, 1298.

[34] Mark J. Isaacson, Frank R. McLarnon and Elton J. Cairns, Zinc electrode rest potentials in concentrated KOH-K2Zn(OH)4 electrolytes, *J. Electrochem. Soc.* **137** (1990), no. 8, 2361–2364.

[35] J. Newman and K. E. Thomas-Alyea, *Electrochemical Systems*, Electrochemical Society Series, Wiley, 2004.

[36] N. Perez, *Electrochemistry and Corrosion Science*, Information Technology: Transmission, Processing & Storage, Springer US, 2004.

[37] Xiaoge Gregory Zhang, *Corrosion and Electrochemistry of Zinc*, 1996.

[38] C. Cachet, U. Ströder and R. Wiart, The kinetics of zinc electrode in alkaline zincate electrolytes, *Electrochim. Acta* **27** (1982), no. 7, 903–908.

[39] Linlin Chen and Andrzej Lasia, Study of the kinetics of hydrogen evolution reaction on nickel-zinc alloy electrodes, *J. Electrochem. Soc.* **138** (1991), no. 11, 3321–3328.

[40] Jan Dundálek, Ivo Šnajdr, Ondřej Libánský, Jiří Vrána, Jaromír Pocedič, Petr Mazúr, et al., Zinc electrodeposition from flowing alkaline zincate solutions: Role of hydrogen evolution reaction, *J. Power Sources* **372** (2017), no. October, 221–226.

[41] C. A. Pino Muñoz, H. Hewa Dewage, V. Yufit and N. P. Brandon, A unit cell model of a regenerative hydrogen-vanadium fuel cell, *J. Electrochem. Soc.* **164** (2017), no. 14, F1717–F1732.

[42] T. Sukkar and M. Skyllas-Kazacos, Water transfer behaviour across cation exchange membranes in the vanadium redox battery, *J. Membr. Sci.* **222** (Sep. 2003), no. 1-2, 235–247.

[43] Catherine Lenihan, Daniela Oboroceanu, Nathan Quill, Deidre Ni Eidhin, Andrea Bourke, Robert Lynch, et al., Water affinity of vanadium electrolytes, *ECS Trans.* **85** (2018), no. 13, 175–189.

[44] R. A. Assink, Fouling mechanism of separator membranes for the iron/chromium redox battery, *J. Membr. Sci.* **17** (1984), no. 2, 205–217.

[45] M. Lopez-Atalaya, G. Codina, J. R. Perez, J. L. Vazquez and A. Aldaz, Optimization studies on a Fe/Cr redox flow battery, *J. Power Sources* **39** (1992), no. 2, 147–154.

[46] Helen Prifti, Aishwarya Parasuraman, Suminto Winardi, Tuti Mariana Lim and Maria Skyllas-Kazacos, Membranes for redox flow battery applications, *Membranes* **2** (2012), no. 2, 275–306.

[47] P. Leung, A. A. Shah, L. Sanz, C. Flox, J. R. Morante, Q. Xu, et al., Recent developments in organic redox flow batteries: A critical review, *J. Power Sources* **360** (2017), 243–283.

[48] Kaixiang Lin, Qing Chen, Michael R. Gerhardt, Liuchuan Tong, Sang Bok Kim, Louise Eisenach, et al., Alkaline quinone flow battery, *Science* **349** (2015), no. 6255, 1529–1532.

[49] Vikram Singh, Soeun Kim, Kang Jungtaek and Hye Ryung Byon, Aqueous organic redox flow batteries, *Nano Res.* **12** (1988–2001), no. 9, 2019.

[50] Arjun Bhattarai, Purna C. Ghimire, Adam Whitehead, Rüdiger Schweiss, Günther G. Scherer, Nyunt Wai, et al., Novel approaches for solving the capacity fade problem during operation of a vanadium redox flow battery, *Batteries* **4** (2018), no. 4, 1–9.

[51] Shuang Gu, Ke Gong, Emily Z. Yan and Yushan Yan, A multiple ion-exchange membrane design for redox flow batteries, *Energy Environ. Sci.* **7** (2014), no. 9, 2986–2998.

[52] Ke Gong, Xiaoya Ma, Kameron M. Conforti, Kevin J. Kuttler, Jonathan B. Grunewald, Kelsey L. Yeager, et al., A zinc-iron redox-flow battery under \$100 per kW h of system capital cost, *Energy Environ. Sci.* **8** (2015), no. 10, 2941–2945.

[53] C. Zhang, J. M. Wang, L. Zhang, J. Q. Zhang and C. N. Cao, The behavior of the amalgamated zinc electrode in supersaturated alkaline zincate solutions, *J. Electrochem. Soc.* **148** (2001), no. 7, 310–312.

[54] J. O. Hill, I. G. Worsley and L. G. Hepler, Thermochemistry and oxidation potentials of vanadium, niobium, and tantalum, *Chem. Rev.* **71** (1971), no. 1, 127.

[55] R. Shivkumar, G. Paruthimal Kalaignan and T. Vasudevan, Effect of additives on zinc electrodes in alkaline battery systems, *J. Power Sources* **55** (1995), no. 1, 53–62.

[56] Aroa R. Mainar, Olatz Leonet, Miguel Bengoechea, Iker Boyano, Iratxe de Meatza, Andriy Kvasha, et al., Alkaline aqueous electrolytes for secondary zinc–air batteries: An overview, *Int. J. Energy Res.* **40** (2016), no. 8, 1032–1049.

[57] T. Roubicek, *Nonlinear Partial Differential Equations with Applications*, International Series of Numerical Mathematics, Birkhäuser Basel, 2005.